Inorg. Chem. **2008**, *47*, 162–175

Self-Assembled Copper(II) Coordination Polymers Derived from Aminopolyalcohols and Benzenepolycarboxylates: Structural and Magnetic Properties

Alexander M. Kirillov,[†] Yauhen Y. Karabach,[†] Matti Haukka,[‡] M. Fátima C. Guedes da Silva,[†,§] Joaquin Sanchiz,[||] Maximilian N. Kopylovich,[†] and Armando J. L. Pombeiro*[,†]

Centro de Química Estrutural, Complexo I, Instituto Superior Técnico, TU Lisbon, Av. Rovisco Pais, 1049-001, Lisbon, Portugal, University of Joensuu, Department of Chemistry, P.O. Box 111, FIN-80101, Joensuu, Finland, Universidade Lusófona de Humanidades e Tecnologias, Av. do Campo Grande, 376, 1749-024, Lisbon, Portugal, Departamento de Química Inorgánica, Universidad de La Laguna, 38200 La Laguna, Tenerife, Spain

Received August 24, 2007

The new copper(II) or copper(II)/sodium(I) 1D coordination polymers $[Cu_2(Hmdea)_2(\mu\text{-}H_2O)(\mu_2\text{-}tpa)]_n \cdot 2nH_2O$ (**1**), $[Cu_2(H_2tipa)_2(\mu_2\text{-}ipa)]_n \cdot 4nH_2O$ (**2**), $[Cu_2(H_2tea)_2Na(H_2O)_2(\mu_2\text{-}tma)]_n \cdot 6nH_2O$ (**3**), $[Cu_2(H_2tea)_2(\mu_2\text{-}ipa)]_n \cdot nH_2O$ (**4a**), and $[Cu_2(H_2tea)_2\{\mu_3\text{-}Na(H_2O)_3\}(\mu_3\text{-}ipa)]_n(NO_3)_n \cdot 0.5nH_2O$ (**4b**) have been prepared in aqueous medium by self-assembly from copper(II) nitrate, aminopolyalcohols [methyldiethanolamine (H_2mdea), triisopropanolamine (H_3tipa), and triethanolamine (H_3tea)] as main chelating ligands and benzenepolycarboxylic acids [terephthalic (H_2tpa), isophthalic (H_2ipa), and trimesic (H_3tma) acid] as spacers. They have been characterized by IR spectroscopy, elemental and single-crystal X-ray diffraction analyses, the latter indicating the formation of unusual multinuclear metal cores interconnected by various benzenepolycarboxylate spacers, leading to distinct wavelike, zigzag, or linear 1D polymeric metal–organic chains. These are further extended to 2D or 3D hydrogen-bonded supramolecular networks via extensive interactions with the intercalated crystallization water molecules. The latter are associated, also with aqua ligands, by hydrogen bonds resulting in acyclic $(H_2O)_3$ clusters in **1**, $(H_2O)_8$ clusters in **2**, infinite 1D water chains in **3**, and disordered water–nitrate associates in **4b**, all playing a key role in the structure stabilization and its extension to further dimensions. Variable-temperature magnetic susceptibility measurements have shown that **1**–**4** exhibit a moderately strong ferromagnetic coupling through the alkoxo bridge. The small Cu–O–Cu bridging angle and the large out-of-plane displacement of the carbon atom of the alkoxo group accounts for this behavior. The magnetic data have been analyzed by means of a dinuclear and a 1D chain model, and the magnetic parameters have been determined. The magnetic exchange coupling in **3**, to our knowledge, is the highest found in alkoxo-bridged copper(II) complexes.

Introduction

The design of copper−organic polymeric molecules is an intensively growing research field in inorganic, coordination, and supramolecular chemistries, which attracts special attention due to the structural and practical characteristics of such materials such as their unpredictable structural diversity, microporosity, interesting molecular sorption, ion exchange, host−guest, magnetic, and catalytic properties, usually different from the related mononuclear species.[1] In particular,

* To whom correspondence should be addressed. E-mail: pombeiro@ist.utl.pt, Phone: +351 218419237, Fax: +351 218464455 (A.J.L.P.).
[†] Instituto Superior Técnico.
[‡] University of Joensuu.
[§] Universidade Lusófona de Humanidades e Tecnologias.
[||] Universidad de La Laguna.

(1) For reviews, see: (a) Biradha, K.; Sarkar, M.; Rajput, L. *Chem. Commun.* **2006**, *40*, 4169. (b) Robin, A. Y.; Fromm, K. M. *Coord. Chem. Rev.* **2006**, *250*, 2127. (c) Kitagawa, S.; Uemura, K. *Chem. Soc. Rev.* **2005**, *34*, 109. (d) Ye, B. H.; Tong, M. L.; Chen, X. M. *Coord. Chem. Rev.* **2005**, *249*, 545. (e) Kitagawa, S.; Kitaura, R.; Noro, S. *Angew. Chem., Int. Ed.* **2004**, *43*, 2334. (f) Rao, C. N. R.; Natarajan, S.; Vaidhyanathan, R. *Angew. Chem., Int. Ed.* **2004**, *43*, 1466. (g) Janiak, C. *Dalton Trans.* **2003**, 2781. (h) Beatty, A. M. *Coord. Chem. Rev.* **2003**, *246*, 131. (i) Moulton, B.; Zaworotko, M. J. *Chem. Rev.* **2001**, *101*, 1629. (j) Eddaoudi, M.; Moler, D. B.; Li, H. L.; Chen, B. L.; Reineke, T. M.; O'Keeffe, M.; Yaghi, O. M. *Acc. Chem. Res.* **2001**, *34*, 319. (k) Hagrman, P. J.; Hagrman, D.; Zubieta, J. *Angew. Chem., Int. Ed.* **1999**, *38*, 2639.

10.1021/ic701669x CCC: $40.75
Published on Web 12/11/2007

different benzenepolycarboxylic acids[2−5] and to a lesser extent aminopolyalcohols[6] are known to be good and versatile building blocks in designing copper−organic polymeric materials with varying topologies. Nevertheless, the examples of heteroligand copper frameworks constructed from both types of these ligands remain very scant.[7]

Recently, we have reported[7,8] the interesting catalytic and host−guest properties of a novel series of multinuclear copper complexes and coordination polymers obtained via self-assembly synthesis (Scheme 1) based on a simple combination, at room temperature, of copper nitrate (metal source), water (solvent), triethanolamine (main chelating ligand), sodium hydroxide (pH regulator), and aromatic mono- or polycarboxylic acid (auxiliary ligand or spacer, respectively). In this respect, the current study aims to extend the generality of this synthetic approach (Scheme 1) to a variety of main chelating ligands and spacers and to show how a slight structural modification of those aminopolyalcohol or aromatic polycarboxylate ligands may lead to distinct topologies and properties of copper-containing polymeric frameworks.

Scheme 1. General Scheme of Self-Assembly Synthesis

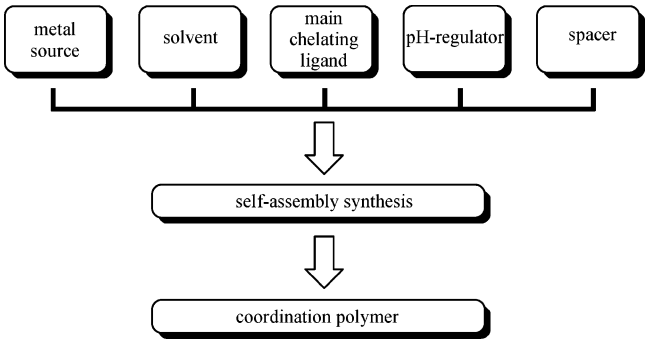

Hence, we report herein the easy self-assembly synthesis, characterization by single-crystal X-ray diffraction, supramolecular features, and magnetic properties of four new coordination polymers **1**−**4** obtained by using methyldiethanolamine (H_2mdea), triisopropanolamine (H_3tipa), or triethanolamine (H_3tea) as main chelating ligands and terephthalic (H_2tpa), isophthalic (H_2ipa), or trimesic (H_3tma) (1,3,5-benzentricarboxylic) acids as spacers. **1**−**4** have distinct polymeric architectures and host different types of water clusters, the latter providing an additional stabilization and/or extension of the 1D metal−organic chains via hydrogen bonds. It is worthwhile to mention that the identification and characterization of water assemblies in various crystalline materials has become an important research field in recent years,[9] namely toward understanding the properties of bulk water as well as the water−water interactions in various environments.

Moreover, our compounds contain alkoxo-bridged copper(II) dinuclear units, which may display interesting magnetic properties. Copper(II) bis(μ-hydroxo) complexes are probably the first examples to offer a clear correlation between their structure and magnetic properties, and they have been widely studied, showing that the exchange coupling constant, J, decreases as the value of the Cu−O−Cu angle is increased. A ferromagnetic coupling takes place for angles smaller than 97.5°, whereas an antiferromagnetic coupling takes place for larger angles.[10] In contrast to the μ-hydroxo complexes, there are just a few magnetostructural studies for alkoxo-bridged copper(II) complexes,[11] and we bring herein such a study for **1**−**4**.

(2) For examples, see the Cambridge Structural Database (CSD, version 5.28, Jan. 2007). Allen, F. H. *Acta Crystallogr.* **2002**, *B58*, 380.

(3) For recent examples with terephthalic acid, see: (a) Hu, T.-L.; Li, J.-R.; Liu, C.-S.; Shi, X.-S.; Zhou, J.-N.; Bu, X.-H.; Ribas, J. *Inorg. Chem.* **2006**, *45*, 162. (b) Du, M.; Jiang, X.-J.; Zhao, X.-J. *Chem. Commun.* **2005**, 5521. (c) Holmes, K. E.; Kelly, P. F.; Dale, S. H.; Elsegood, M. R. J. *CrystEngComm* **2005**, *7*, 202. (d) Paul, B.; Zimmermann, B.; Fromm, K. M.; Janiak, C. *Z. Anorg. Allg. Chem.* **2004**, *630*, 1650. (e) Mukherjee, P. S.; Ghoshal, D.; Zangrando, E.; Mallah, T.; Chaudhuri, N. R. *Eur. J. Inorg. Chem.* **2004**, 4675. (f) Hong, C. S.; You, Y. S. *Polyhedron* **2004**, *23*, 3043.

(4) For recent examples with isophthalic acid, see: (a) Shen, W.-Z.; Chen, X.-Y.; Cheng, P.; Yan, S.-P.; Zhai, B.; Liao, D.-Z.; Jiang, Z.-H. *Eur. J. Inorg. Chem.* **2005**, 2297. (b) Wen, Y.-H.; Cheng, J.-K.; Feng, Y.-L.; Zhang, J.; Li, Z.-J.; Yao, Y.-G. *Inorg. Chim. Acta* **2005**, *358*, 3347. (c) Zhou, Y.-F.; Jiang, F.-L.; Yuan, D.-Q.; Wu, B.-L.; Wang, R.-H.; Lin, Z.-Z.; Hong, M.-C. *Angew. Chem., Int. Ed.* **2004**, *43*, 5665. (d) Cheng, P.; Yan, S.-P.; Xie, C.-Z.; Zhao, B.; Chen, X.-Y.; Liu, X.-W.; Li, C.-H.; Liao, D.-Z.; Jiang, Z.-H.; Wang, G.-L. *Eur. J. Inorg. Chem.* **2004**, 2369. (e) Wen, Y.-H.; Cheng, J.-K.; Zhang, J.; Li, Z.-J.; Kang, Y.; Yao, Y.-G. *Inorg. Chem. Commun.* **2004**, *7*, 1120. (f) Moulton, B.; Abourahma, H.; Bradner, M. W.; Lu, J.; McManus, G. J.; Zaworotko, M. J. *Chem. Commun.* **2003**, 1342. (g) Abourahma, H.; Bodwell, G. J.; Lu, J.; Moulton, B.; Pottie, I. R.; Walsh, R. B.; Zaworotko, M. J. *Cryst. Growth Des.* **2003**, *3*, 513.

(5) For recent examples with trimesic acid, see: (a) Yang, J.; Ma, J.-F.; Liu, Y.-Y.; Ma, J.-C.; Jia, H.-Q.; Hu, N.-H. *Eur. J. Inorg. Chem.* **2006**, 1208. (b) Gheorghe, R.; Cucos, P.; Andruh, M.; Costes, J.-P.; Donnadieu, B.; Shova, S. *Chem.−Eur. J.* **2006**, *12*, 187. (c) Wang, P.; Moorefield, C. N.; Panzer, M.; Newkome, G. R. *Chem. Commun.* **2005**, 465. (d) Konar, S.; Mukherjee, P. S.; Zangrando, E.; Drew, M. G. B.; Diaz, C.; Ribas, J.; Chaudhuri, N. R. *Inorg. Chim. Acta* **2005**, *358*, 29. (e) Holmes, K. E.; Kelly, P. F.; Elsegood, M. R. J. *Dalton Trans.* **2004**, 3488. (f) Yang, L.; Naruke, H.; Yamase, T. *Inorg. Chem. Commun.* **2003**, *6*, 1020.

(6) (a) Marin, G.; Tudor, V.; Kravtsov, V. C.; Schmidtmann, M.; Simonov, Y. A.; Muller, A.; Andruh, M. *Cryst. Growth Des.* **2005**, *5*, 279. (b) Escovar, R. M.; Thurston, J. H.; Ould-Ely, T.; Kumar, A.; Whitmire, K. H. *Z. Anorg. Allg. Chem.* **2005**, *631*, 2867. (c) Chen, F.-T.; Li, D.-F.; Gao, S.; Wang, X.-Y.; Li, Y.-Z.; Zheng, L.-M.; Tang, W.-X. *Dalton Trans.* **2003**, 3283. (d) Tudor, V.; Marin, G.; Kravtsov, V.; Simonov, Y. A.; Lipkowski, J.; Brezeanu, M.; Andruh, M. *Inorg. Chim. Acta* **2003**, *353*, 35. (e) Yamaguchi, H.; Inomata, Y.; Takeuchi, T. *Inorg. Chim. Acta* **1990**, *172*, 105. (f) Yamaguchi, H.; Inomata, Y.; Takeuchi, T. *Inorg. Chim. Acta* **1989**, *161*, 217.

(7) (a) Kirillov, A. M.; Kopylovich, M. N.; Kirillova, M. V.; Haukka, M.; da Silva, M. F. C. G.; Pombeiro, A. J. L. *Angew. Chem., Int. Ed.* **2005**, *44*, 4345. (b) Karabach, Y. Y.; Kirillov, A. M.; da Silva, M. F. C. G.; Kopylovich, M. N.; Pombeiro, A. J. L. *Cryst. Growth Des.* **2006**, *6*, 2200.

(8) Kirillov, A. M.; Kopylovich, M. N.; Kirillova, M. V.; Karabach, E. Y.; Haukka, M.; da Silva, M. F. C. G.; Pombeiro, A. J. L. *Adv. Synth. Catal.* **2006**, *348*, 159.

(9) (a) Mascal, M.; Infantes, L.; Chisholm, J. *Angew. Chem., Int. Ed.* **2006**, *45*, 32. (b) Infantes, L.; Motherwell, S. *CrystEngComm* **2002**, *4*, 454. (c) Infantes, L.; Chisholm, J.; Motherwell, S. *CrystEngComm* **2003**, *5*, 480. (d) Ludwig, R. *Angew. Chem., Int. Ed.* **2001**, *40*, 1808. (e) Supriya, S.; Das, S. K. *J. Cluster Sci.* **2003**, *14*, 337. (f) Bergougnant, R. D.; Robin, A. Y.; Fromm, K. M. *Cryst. Growth Des.* **2005**, *5*, 1691.

(10) (a) Crawford, V. H.; Richardson, H. W.; Wasson, J. R.; Hodgson, D. J.; Hatfield, W. E. *Inorg. Chem.* **1976**, *15*, 2107. (b) Kahn, O. *Molecular Magnetism*, VCH: New York, Weinheim and Cambridge, 1993.

(11) (a) Ruiz, E.; Alemany, P.; Alvarez, S.; Cano, J. *J. Am. Chem. Soc.* **1997**, *119*, 1297. (b) Ruiz, E.; Alemany, P.; Alvarez, S.; Cano, J. *Inorg. Chem.* **1997**, *36*, 3683. (c) Doyle, R. P.; Julve, M.; Lloret, F.; Nieuwenhuyzen, M.; Kruger, P. *Dalton Trans.* **2006**, 2081.

Experimental Section

Materials and Methods. All of the synthetic work was performed in air and at room temperature. All of the chemicals were obtained from commercial sources and used as received. Carbon, hydrogen, and nitrogen elemental analyses were carried out by the Microanalytical Service of the Instituto Superior Técnico. Melting points were determined on a Kofler table. Infrared spectra (4000−400 cm^{-1}) were recorded on a BIO-RAD FTS 3000MX instrument in KBr pellets. Magnetic susceptibility measurements on polycrystalline samples were carried out in the temperature range 2.0−300 K by means of a Quantum Design SQUID magnetometer operating at 500 Oe (T < 15 K) and 10 000 Oe (T > 15 K). Diamagnetic corrections of the constituent atoms were estimated from Pascal's constants as -244.23×10^{-6}, -305.1×10^{-6}, -335.9×10^{-6}, and -254.3×10^{-6} $cm^3\ mol^{-1}$ for **1**, **2**, **3**, and **4a** respectively. Experimental susceptibilities were also corrected for the temperature-independent paramagnetism [60×10^{-6} $cm^3\ mol^{-1}$ *per* copper(II)] and the magnetization of the sample holder.

General Synthetic Procedure for 1−4. To an aqueous solution (10.0 mL) containing $Cu(NO_3)_2 \cdot 2.5H_2O$ (1.00 mmol) in HNO_3 (1.00 mmol) [the acid was added to avoid spontaneous hydrolysis of the metal salt] were added dropwise the aminopolyalcohol (1.00 mmol) [methyldiethanolamine (115 μL) for **1**, triisopropanolamine (191 mg) for **2**, triethanolamine (130 μL) for **3** and **4**], an aqueous solution (3.0 mL) of NaOH (120 mg, 3.00 mmol) and benzenepolycarboxylic acid [terephthalic acid (83 mg, 0.50 mmol) for **1**, isophthalic acid (83 mg, 0.50 mmol) for **2** and **4**, and trimesic acid (69 mg, 0.33 mmol) for **3**] in this order and with continuous stirring at room temperature. The resulting reaction mixture was stirred overnight and then filtered off. The filtrate was left to evaporate in a beaker at ambient (ca. 20−25 °C) temperature. Blue X-ray quality crystals of **1**, **2**, **3**, and **4a** in ca. 50% yield (based on copper nitrate) were formed in 1−2 weeks and then collected and dried in air.

$[Cu_2(Hmdea)_2(\mu\text{-}H_2O)(\mu_2\text{-}tpa)]_n \cdot 2nH_2O$ (1). IR (KBr): ν = 3398 (s br) and 3240 (s br) ν(OH)+ν(H_2O), 2981 (w) ν_{as}(CH), 2908 (w) and 2866 (w) ν_s(CH), 1655 (w sh) and 1574 (s) ν_{as}(COO), 1385 (s) ν_s(COO), 1060 (m) cm^{-1} ν(C−O); elemental analysis Calcd (%) for $C_{18}H_{34}Cu_2N_2O_{11}$ (581.6): C 37.17, H 5.89, N 4.81; found C 37.21, H 5.93, N 4.91.

$[Cu_2(H_2tipa)_2(\mu_2\text{-}ipa)]_n \cdot 4nH_2O$ (2). IR (KBr): ν = 3428 (s br) and 3235 (m br) ν(OH)+ν(H_2O), 2976 (m) ν_{as}(CH), 2922 (w) and 2877 (m) ν_s(CH), 1650 (w sh), 1606 (s) and 1557 (s) ν_{as}(COO), 1436 (m) and 1381 (s) ν_s(COO), 1127 (m) cm^{-1} ν(C−O); elemental analysis Calcd (%) for $C_{26}H_{52}Cu_2N_2O_{14}$ (743.8): C 41.98, H 7.04, N 3.77; found C 41.56, H 7.23, N 3.82.

$[Cu_2(H_2tea)_2Na(H_2O)_2(\mu_2\text{-}tma)]_n \cdot 6nH_2O$ (3). IR (KBr): ν = 3491 (s br), 3398 (s br) and 3263 (s br) ν(OH)+ν(H_2O), 2967 (w) ν_{as}(CH), 2919 (m) and 2871 (m) ν_s(CH), 1660 (w sh), 1609 (s) and 1555 (s) ν_{as}(COO), 1434 (s) and 1369 (s) ν_s(COO), 1082 (m) and 1066 (m) cm^{-1} ν(C−O); elemental analysis Calcd (%) for $C_{21}H_{49}Cu_2NaN_2O_{20}$ (799.7): C 31.54, H 6.17, N 3.50; found C 31.68, H 6.18, N 3.65.

$[Cu_2(H_2tea)_2(\mu_2\text{-}ipa)]_n \cdot nH_2O$ (4a). IR (KBr): ν = 3530 (s br), 3356 (s br) and 3255 (s br) ν(OH)+ν(H_2O), 2964 (m) ν_{as}(CH), 2880 (m) and 2853 (m) ν_s(CH), 1675 (w sh), 1604 (s) and 1556 (s) ν_{as}(COO), 1453 (m) and 1382 (s) ν_s(COO), 1093 (m) ν(C−O); elemental analysis Calcd (%) for $C_{20}H_{34}Cu_2N_2O_{11}$ (605.6): C 39.67, H 5.66, N 4.63; found C 39.36, H 5.59, N 4.65. A slow evaporation of the reaction mixture of **4** at a slightly lower temperature (ca. 10−15 °C) led to the formation of a mixture of **4a** (main product) with the derived compound $[Cu_2(H_2tea)_2\{\mu_3\text{-}Na(H_2O)_3\}(\mu_3\text{-}ipa)]_n(NO_3)_n \cdot 0.5nH_2O$ (**4b**) (minor product) isolated as blue X-ray quality crystals. **4b** displays an IR spectrum that is almost equal to that of **4a**. (**4b**): IR (KBr): ν = 3490 (sh), 3401 (s br) and 3255 (s br) ν(OH)+ν(H_2O), 2964 (m) ν_{as}(CH), 2880 (m) and 2854 (m) ν_s(CH), 1676 (w sh), 1605 (s) and 1555 (s) ν_{as}(COO), 1452 (m) and 1381 (s) ν_s(COO), 1092 (m) ν(C−O).

X-ray Crystallography. For **2**, **3**, and **4b**, the X-ray diffraction data were collected with a Nonius Kappa CCD diffractometer using Mo Kα radiation. Crystals were mounted in inert oil within the cold gas stream of the diffractometer. The *DENZOSCALEPACK* program package[12] was used for cell refinements and data reductions. The structures were solved by direct methods using the *SHELXS-97* program.[13] An empirical absorption correction was applied to **2** and **3** using *XPREP* in *SHELXTL* version 6.14−1 or *SADABS* version 2.10 programs.[14a,b] An analytical absorption correction (de Meulenaer Tompa)[14c] was applied to **4b**. Structural refinements were carried out with the *SHELXL-97* program.[15] In **2**, one of the water molecules was disordered over two sites (O14A and O14B) with equal occupancies. Another water molecule (O11) was partially lost and refined with an occupancy of 0.5. The moiety of C23, C24, C25, and O7 was also disordered over two orientations with occupancies of 0.65 and 0.35, thus accounting for the residual electron density in **2**. These atoms were restrained so that their U_{ij} components approximate to isotropic behavior. Anisotropic refinement or expansion of the disorder model did not improve the structure model of **2**. The residual electron density in **4b** is due to the disorder over two sites of two nitrate moieties (N1, O14, O15, O16 and N2, O17, O18, O19) and one water molecule (O20). These atoms were also restrained so that their U_{ij} components approximate to isotropic behavior. Furthermore, the OH group (O3) was restrained to approximate isotropic behavior as well. No acceptable disorder model could be applied for this atom. The H_2O and OH hydrogen atoms in **2**−**4** were located from the difference Fourier map but constrained to ride on their parent atom, with U_{iso} = 1.5 U_{eq} (parent atom). Other hydrogen atoms were positioned geometrically and were also constrained to ride on their parent atoms, with C−H = 0.95−0.99 Å and U_{iso} = 1.2−1.5 U_{eq} (parent atom).

For **4a**, the intensity data were collected using a Bruker AXS-KAPPA APEX II diffractometer with graphite monochromated Mo Kα radiation. Data were collected at 150 K using omega scans of 0.5° per frame, and a full sphere of data was obtained. Cell parameters were retrieved using Bruker *SMART* software and refined using Bruker *SAINT* on all of the observed reflections. Absorption corrections were applied using *SADABS*. Structures were solved by direct methods by using the *SHELXS−97* package[13] and refined with *SHELXL−97*[15] with the WinGX graphical user interface.[16] All of the hydrogens were inserted in calculated positions.

For **1**, the X-ray diffraction data were collected on an Enraf-Nonius CAD4 diffractometer, equipped with a graphite monochromator and using Mo Kα radiation (λ = 0.71069 Å). The structure was solved by direct methods using the *SHELXS-97* package.[13] An empirical absorption correction based on equivalent reflections was

(12) Otwinowski, Z.; Minor, W. *Methods in Enzymology*, Macromolecular Crystallography, Part A; Carter, C. W., Jr, Sweet, R. M., Eds.; Academic Press: New York, 1997; Vol. 276, pp 307−326.
(13) Sheldrick, G. M. *SHELXS-97, Program for Crystal Structure Determination*; University of Göttingen: Göttingen, Germany, 1997.
(14) (a) Sheldrick, G. M. *SHELXTL*, ver. 6.14−1; Bruker AXS Inc.: Madison, Wisconsin, U.S.A., 2005. (b) Sheldrick, G. M. *SADABS - Bruker Nonius scaling and absorption correction*, ver. 2.10; Bruker Axs Inc., Madison, Wisconsin, U.S.A., 2003. (c) de Meulenaer, J.; Tompa, H. *Acta Crystallogr.* **1965**, *19*, 1014.
(15) Sheldrick, G. M. *SHELXL97*, University of Göttingen: Göttingen, Germany, 1997.
(16) Farrugia, L. J. *J. Appl. Crystallogr.* **1999**, *32*, 837.

Table 1. Crystal Data and Structure Refinement Details for **1**−**4**

	1	**2**	**3**	**4a**	**4b**
empirical formula	$C_{18}H_{34}Cu_2N_2O_{11}$	$C_{26}H_{51}Cu_2N_2O_{13.5}$	$C_{21}H_{47}Cu_2NaN_2O_{20}$	$C_{20}H_{34}Cu_2N_2O_{11}$	$C_{80}H_{156}Cu_8N_{12}Na_4O_{66}$
fw	581.57	734.77	797.68	605.57	2942.45
T (K)	291(2)	120(2)	120(2)	150(2)	120(2)
λ (Å)	0.71073	0.71073	0.71073	0.71069	0.71073
cryst syst	monoclinic	monoclinic	orthorhombic	orthorhombic	monoclinic
space group	*P*2/*C*	*P*2$_1$/*n*	*Pbcn*	*Pbca*	*P*21/*c*
a (Å)	10.751(2)	9.9893(4)	14.6973(2)	13.8183(6)	12.4289(3)
b (Å)	6.9767(10)	22.7320(7)	17.7243(5)	13.5374(7)	14.3925(6)
c (Å)	16.377(2)	15.0150(6)	12.4624(3)	25.9622(12)	17.9428(7)
α (deg)	90	90	90	90	90
β (deg)	100.653(7)	95.472(2)	90	90	98.631(2)
γ (deg)	90	90	90	90	90
V (Å^3)	1207.1(3)	3394.0(2)	3246.45(13)	4856.6(4)	3173.3(2)
Z	2	4	4	8	1
ρ_{calcd} (mg/m^3)	1.600	1.438	1.664	1.656	1.540
μ(Mo Kα) (mm^{-1})	1.820	1.316	1.409	1.813	1.428
Θ limits (deg)	2.88−25.02	2.24−25.00	2.82−27.48	2.63−25.35	3.73−25.00
completeness (%)	99.9	99.9	99.5	99.9	99.5
no. of collected reflns	2257	49 250	52 474	30 195	24 592
no. of unique reflns	2136	5973	3713	4451	5558
R_{Int}	0.0271	0.1249	0.0734	0.0606	0.0544
no. of params	186	452	240	340	432
Final R1[a], wR2[b] ($I \geq 2\sigma$)	0.0627, 0.0989	0.0572, 0.1370	0.0325, 0.0724	0.0301, 0.0658	0.0638, 0.1832
R1, wR2 (all data)	0.1362, 0.1191	0.0953, 0.1542	0.0510, 0.0803	0.0436, 0.0696	0.0791, 0.1980
GOF on F^2	1.019	1.033	1.063	0.981	1.050
largest diff. peak and hole (e Å^{-3})	0.369, −0.480	1.236, −0.611	0.539, −0.499	0.568; −0.298	1.314, −0.614

[a] $R1 = \sum||F_o| - |F_c||/\sum|F_o|$. [b] $wR2 = [\sum[w(F_o^2 - F_c^2)^2]/\sum[w(F_o^2)^2]]^{1/2}$.

applied. The structure was refined with the *SHELXL-97* program.[16] All of the hydrogens were inserted in calculated positions. A disorder model was included for the methyl carbon C31 as well as for the methylene carbon atoms C21 and C11.

Crystal data and details of data collection for **1**−**4** are reported in Table 1.

Results and Discussion

Synthesis and Spectroscopic Characterization. The copper(II) compounds **1**−**4** have been synthesized via the self-assembly method depicted in Scheme 1. Hence, the simple combination, at room temperature and in air, of copper(II) nitrate as the metal source with water as the solvent and an aminopolyalcohol [i.e., methyldiethanolamine (H_2mdea) for **1**, triisopropanolamine (H_3tipa) for **2**, or triethanolamine (H_3tea) for **3** and **4**] as the main chelating ligand, followed by the alkalization with sodium hydroxide (pH-regulator) and the addition of a benzenepolycarboxylic acid [i.e., terephthalic acid (H_2tpa) for **1**, isophthalic acid (H_2ipa) for **2** and **4**, or trimesic (H_3tma) acid for **3**] as a spacer, provides the self-assembly formation of the new polymeric compounds $[Cu_2(Hmdea)_2(\mu\text{-}H_2O)(\mu_2\text{-tpa})]_n{\cdot}2nH_2O$ (**1**), $[Cu_2(H_2tipa)_2(\mu_2\text{-ipa})]_n{\cdot}4nH_2O$ (**2**), $[Cu_2(H_2tea)_2Na(H_2O)_2\text{-}(\mu_2\text{-tma})]_n{\cdot}6nH_2O$ (**3**), and $[Cu_2(H_2tea)_2(\mu_2\text{-ipa})]_n{\cdot}nH_2O$ (**4a**) (Scheme 2). These products were isolated as blue crystalline solids in ca. 50% yields (based on copper(II) nitrate) and characterized by IR spectroscopy and elemental and single-crystal X-ray diffraction analyses. Besides, slightly different crystallization conditions from those of **4a** lead to the formation of the derived compound $[Cu_2(H_2tea)_2\{\mu_3\text{-}Na(H_2O)_3\}(\mu_3\text{-ipa})]_n(NO_3)_n{\cdot}0.5nH_2O$ (**4b**) (minor product), which additionally comprises an aquasodium moiety (from sodium hydroxide) and a nitrate counterion (Scheme 2). All of the coordination polymers **1**−**4** are stable in air and insoluble in water as well as common organic solvents. It is interesting to mention that in spite of the ionic nature, **4b** appears to be insoluble in water, unlike the related copper(II)/Na(I) coordination polymer $[Cu_2(H_2tea)_2\{\mu_3\text{-}Na_2(H_2O)_4\}(\mu_6\text{-pma})]_n{\cdot}10nH_2O$ (H_4pma = pyromellitic acid).[7b] Upon heating, all of the compounds are fractured and discolored between 70 and 140 °C because of dehydration followed by gradual turning to opaque and decomposition within a broad interval of temperatures starting at above ca. 200 °C.

The IR spectra of **1**−**4** possess related features showing typical vibrations due to the aminopolyalcohol ligands, benzenepolycarboxylate moieties, crystallization, and coordinated water molecules. Thus, the strong and broad bands, typically with two maxima at ca. 3530−3400 and 3260−3235 cm^{-1}, are assigned to the stretching vibrations of OH groups and H_2O molecules. The broad character of the latter and the high intensity is indicative of extensive hydrogen bonding involving OH groups and water. Several weak or medium-intensity ν(CH) bands are also observed with maxima in the 2980−2965, 2920−2910, and 2880−2850 cm^{-1} ranges. The ν_{as} and ν_s vibrations of carboxylate groups are detected as two (in **1**) or four (in **2**−**4**) high- or medium-intensity bands with absorbance maxima in the 1610−1555 and 1455−1370 cm^{-1} ranges, respectively, also having shoulders in the 1675−1650 cm^{-1} region. The unprotonated character of one uncoordinated COO^- group in the tma moiety of **3** (Scheme 2) can also be confirmed by the absence of an absorption maximum at around 1730 cm^{-1},[17] which is typical for a protonated COOH group. The elemental analyses of **1**−**4** confirm their analytical purity and are

(17) Cao, R.; Shi, Q.; Sun, D.; Hong, M.; Bi, W.; Zhao, Y. *Inorg. Chem.* **2002**, *41*, 6161.

Scheme 2. Schematic Representations (Repeating Units) of **1**−**4**[a]

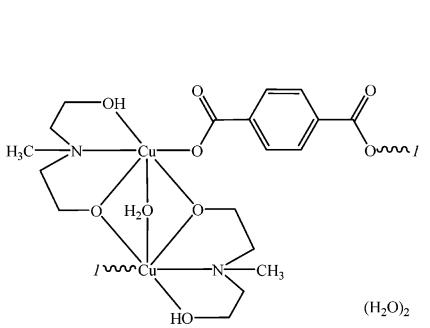

$[Cu_2(Hmdea)_2(\mu\text{-}H_2O)(\mu_2\text{-}tpa)]_n\cdot 2nH_2O$ (**1**)

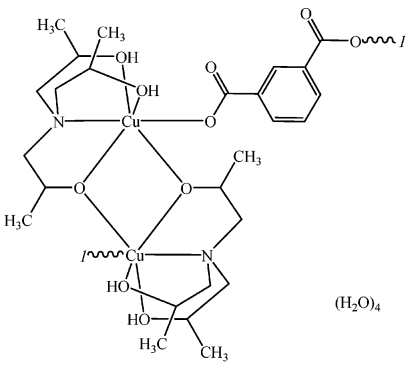

$[Cu_2(H_2tipa)_2(\mu_2\text{-}ipa)]_n\cdot 4nH_2O$ (**2**)

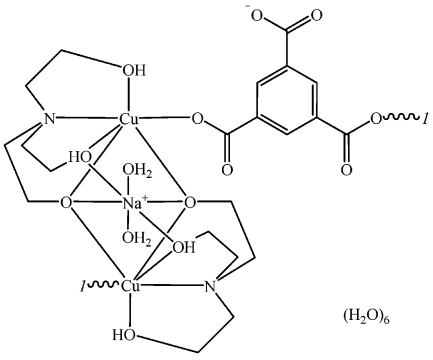

$[Cu_2(H_2tea)_2Na(H_2O)_2(\mu_2\text{-}tma)]_n\cdot 6nH_2O$ (**3**)

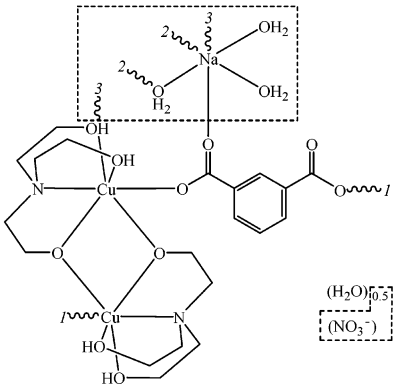

$[Cu_2(H_2tea)_2(\mu_2\text{-}ipa)]_n\cdot nH_2O$ (**4a**) (without the fragments within the dotted rectangles); $[Cu_2(H_2tea)_2\{\mu_3\text{-}Na(H_2O)_3\}(\mu_3\text{-}ipa)]_n(NO_3)_n\cdot 0.5nH_2O$ (**4b**) (with those fragments)

[a] Numbers indicate the corresponding extensions of polynuclear chains.

consistent with formulations (Scheme 2) authenticated by the X-ray diffraction studies, as indicated below.

Basic Description of X-ray Crystal Structures. The X-ray crystal analyses reveal that **1**−**4** possess 1D infinite polymeric architectures constructed from dinuclear $[Cu_2(aminopolyalcohol)_2]^{2+}$ units, which are interconnected by benzenepolycarboxylate ligands acting as spacers (Scheme 2). The structures of **3** and **4b** also reveal an additional incorporation of aqua sodium moieties, leading to the formation of an heterometallic copper/sodium framework. The displacement ellipsoid plots for structural fragments of **1**−**4** are depicted in Figure 1, whereas the partial-crystal packing diagrams exhibiting metal−organic polymeric chains are shown in Figure 2. The selected bonding parameters and hydrogen-bonding distances [*d*(D···A)] are given in Tables 2 and 3, respectively. All of the symmetry codes along the discussion below are those of Tables 2 and 3.

$[Cu_2(Hmdea)_2(\mu\text{-}H_2O)(\mu_2\text{-}tpa)]_n\cdot 2nH_2O$ (1). The molecular structure of **1** (part a of Figure 1) contains the centrosymmetric binuclear $[Cu_2(Hmdea)_2(\mu\text{-}H_2O)]^{2+}$ fragments stabilized by bound μ_2-terephthalate anions, thus forming the wavelike metal−organic chains (part a of Figure 2). Each Cu1 atom has a distorted tetragonal-bipyramidal geometry filled by a tridentate Hmdea ligand with one bridging alkoxo group (O12), one terephthalate oxygen atom (O1), and one bridging water molecule (O10). The binding of the Hmdea ligand involves two five-membered chelate rings with bite N1−Cu1−O12 and N1−Cu1−O22 angles of 85.5(2) and 78.9(2)°, respectively. The Cu1−O12 [1.948(4) Å] and Cu1−O1 [1.930(5) Å] bond lengths (Table 2) are within typical values for Cu−μO and Cu−O(tpa) bonds,[18] whereas the Cu1−O22 [2.510(6) Å] and Cu1−O10 [2.566(7) Å] distances are remarkably longer than the average bonds of that type but are comparable to those reported previously for some compounds.[6b,d,7,8,19a] The binding of the terephthalate moiety is additionally stabilized by the intramolecular O22−H22···O2 [2.678(7) Å] hydrogen bond (part a of Figure 1, Table 3) between an OH group of Hmdea and the free carboxylate oxygen. The bridging O12 and O10 atoms are involved in the generation of an unusual $[Cu_2(\mu\text{-}O)_2(\mu\text{-}H_2O)]$ core with a cocked-hat-like geometry (part a of Figure 3), in which the centrosymmetric $[Cu_2(\mu\text{-}O)_2]$ unit is nonplanar, having both O12 atoms shifted in the opposite direction relatively to the apical water molecule O10. The Cu···Cu separation within that core is 2.793(6) Å, whereas the representative O12−Cu1−O12^i, Cu1−O10−Cu1^i, and Cu1−O12−Cu1^i bond angles are 80.30(15), 66.0(2), and 91.27(15)°, respectively (Table 2). It is worthwhile to

(18) Orpen, A. G.; Brammer, L.; Allen, F. H.; Kennard, O.; Watson, D. G.; Taylor, R. *J. Chem. Soc., Dalton Trans.* **1989**, S1.

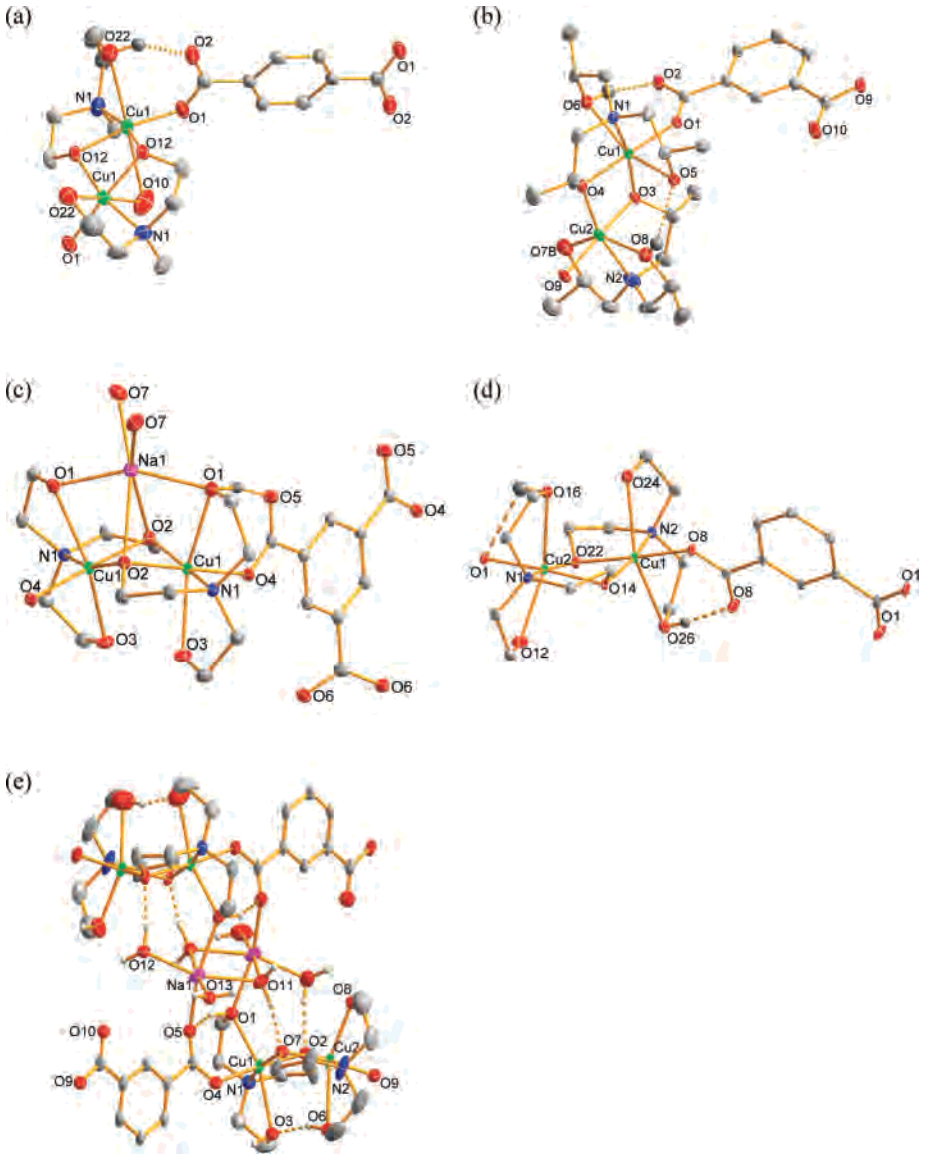

Figure 1. Structural fragments of **1** (a), **2** (b), **3** (c), **4a** (d), and **4b** (e) with the partial atom labeling scheme and intramolecular hydrogen bonds (dashed lines). Hydrogen atoms (apart from those involved in hydrogen bonds), crystallization water molecules, and counter-ions are omitted for clarity. Displacement ellipsoids are drawn at the 30 (a, b, e) or 50% (c, d) probability level. Copper, green; sodium, purple; nitrogen, blue; oxygen, red; carbon, gray.

mention that the now encountered $[Cu_2(\mu\text{-}O)_2(\mu\text{-}H_2O)]$ core in **1**, with the μ-H_2O ligand completing the coordination sphere of both copper atoms, appears to be the first reported example of that type, although there are plenty of structures with a simpler $[Cu_2(\mu\text{-}O)_2]$ unit[2] and only three compounds known[19] with the related $[Cu_2(\mu\text{-}OH)_2(\mu\text{-}H_2O)]$ fragment. Moreover, to our knowledge,[2] **1** seems to constitute the first transition-metal coordination polymer derived from methyldiethanolamine.

$[Cu_2(H_2tipa)_2(\mu_2\text{-ipa})]_n \cdot 4nH_2O$ (2). The crystal structure of **2** (part b of Figure 1) consists of asymmetric dimeric units $[Cu_2(H_2tipa)_2]^{2+}$ linked by bridging μ_2-ipa ligands, leading to zigzag-type metal−organic chains (part b of Figure 2). Triisopropanolamine is monodeprotonated and acts as a tetradentate ligand. Both Cu1 and Cu2 atoms exhibit distorted tetragonal bipyramidal geometries. The equatorial planes are formed by two bridging alkoxo oxygen atoms (O3 and O4), amino nitrogen atoms (N1 and N2), and isophthalate (O1 and O9) atoms, whereas the remaining H_2tipa oxygen atoms O5, O6, O7, and O8 are located in apical positions. As in **1**, the latter have significantly longer distances [Cu1−O5 and Cu1−O6 of 2.577(4) and 2.459(4) Å, respectively] than, for example, Cu1−O3 [1.936(4) Å] and Cu1−O1 [1.966(3) Å] bonds (Table 2). The $[Cu_2(\mu\text{-}O)_2]$ core with the Cu···Cu separation of 2.886(1) Å is nonplanar, showing a twisted-square geometry (part b of Figure 3). The intramolecular O(6)−H(6O)···O(2) [2.677(5) Å] and O(7)−H(7)···O(10) [av 2.634(16) Å] hydrogen bonds (part b of Figure 1, Table 3) between OH groups of H_2tipa and free isophthalate oxygen atoms provide their further linkage, forming the six-membered Cu1−O6−H60···O2−C1−O1 and Cu2−O7−H7···O10−C26−O9 rings with the O6−Cu1−O1 [89.89-

(19) (a) El Fallah, M. S.; Escuer, A.; Vicente, R.; Badyine, F.; Solans, X.; Font-Bardia, M. *Inorg. Chem.* **2004**, *43*, 7218. (b) Youngme, S.; van Albada, G. A.; Roubeau, O.; Pakawatchai, C.; Chaichit, N.; Reedijk, J. *Inorg. Chim. Acta* **2003**, *342*, 48. (c) Wu, L.-P.; Keniry, M. E.; Hathaway, B. *Acta Crystallogr.* **1992**, *C48*, 35.

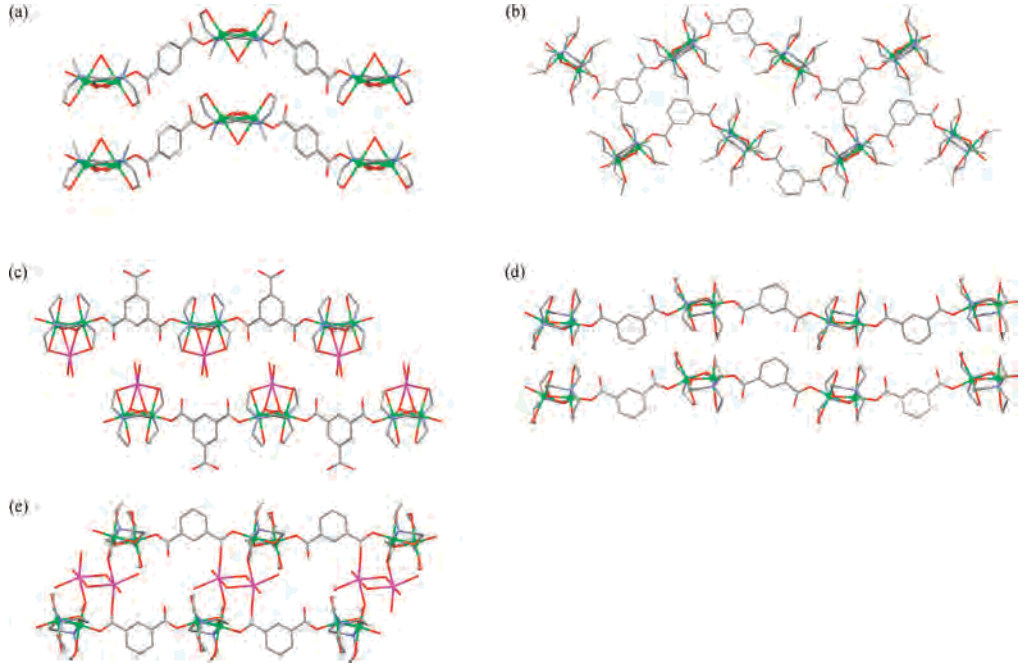

Figure 2. Fragments of the crystal packing diagrams (arbitrary views) of **1** (a), **2** (b), **3** (c), **4a** (d), and **4b** (e) showing two metal−organic chains in **1**, **2**, **3**, and **4a** or one double metal−organic chain in **4b**. Hydrogen atoms, crystallization water molecules and counter-ions are omitted for clarity. Copper, green; sodium, purple; nitrogen, blue; oxygen, red; carbon, gray.

(13)°] and O7−Cu2−O9 [av 89.20(4)°] angles, respectively. Another intramolecular O(8)−H(8O)···O(5) [2.716(5) Å] hydrogen bond is detected between OH groups of two H_2-tipa ligands. In general, most of the bonding parameters in **2** are comparable to those of **1** and other previously reported compounds bearing isophthalate moieties.[4] It should be mentioned that up to date there are only a few structurally characterized coordination compounds with H_3tipa or a derived ligand,[2] in spite of its commercial availability, cheapness, and somehow similarity to the widely used triethanolamine that possesses a rather rich coordination chemistry.[2,6b−d,7,8] Hence, **2**, apart from being the first example of a metal−organic framework derived from H_3-tipa, extends to copper the still-limited number of triisopropanolaminate complexes.

$[Cu_2(H_2tea)_2Na(H_2O)_2(\mu_2\text{-tma})]_n\cdot 6nH_2O$ (3). The unusual feature of the molecular structure of **3** (part c of Figure 1) consists of the additional incorporation of the sodium $[Na(H_2O)_2]^+$ moiety to the typical dimeric copper triethanolaminate $[Cu_2(H_2tea)_2]^{2+}$ unit, thus forming the heterotrimetallic $[Cu_2(H_2tea)_2Na(H_2O)_2]^{3+}$ fragment, which is stabilized by the benzene-1,3,5-tricarboxylate(3-) (trimesate) ligand acting in a μ_2-bridging mode and leading to the linear metal−organic chains (part c of Figure 2). The geometry around the hexacoordinated copper atoms is distorted tetragonal bipyramidal, whereas the sodium atom shares the edges in a significantly distorted octahedral-like structural fashion. Tetradentate triethanolaminate ligands are monodeprotonated at the bridging O2 oxygen atoms[20] which occupy, along with amino nitrogen atoms N1 and carboxylate oxygen atoms O4,[20] the equatorial planes of the $[Cu_2(H_2tea)_2]^{2+}$ unit, whereas the other O1 and O3 oxygen atoms[20] of H_2tea lie in apical positions. The bonding parameters within the $[Cu_2(H_2tea)_2]^{2+}$ unit (Table 2) are comparable to the corresponding ones in **1** and **2** as well as in other copper triethanolaminate complexes.[6b,d,7,8] The four-fold linkage of the sodium ion with both copper atoms is achieved via two O1 and two O2 oxygen atoms of H_2tea with the corresponding Na1−O1 and Na1−O2 bond lengths of 2.3528(16) and 2.6196(19) Å, respectively. The representative O1−Na1−$O1^{ii}$ [154.68(10)°] and O2−Na1−$O2^{ii}$ [56.53(7)°] bond angles defining the binding of the Na1 atom are indicative of significant octahedral-like distortions (Table 2). The coordination sphere of the sodium ion is completed by two terminal aqua ligands (O7)[20] disposed in the cis position, with Na1−O7 distances of 2.387(2) Å and an O7−Na1−$O7^{ii}$ angle of 84.5(10)°. In the resulting heterotrimetallic $[Cu_2(H_2tea)_2Na(H_2O)_2]^{3+}$ fragment, the unusual $[Cu_2(\mu_2\text{-}O)_2(\mu\text{-}O)_2Na]$ core possesses a crownlike geometry (Figure 3) and appears to be the first example of that type in any copper/sodium compounds reported previously.[2] Within that core, the $[Cu_2(\mu_2\text{-}O)_2]$ unit is nonplanar with both μ_2-O atoms shifted toward the apical sodium ion. The Cu···Cu and Cu···Na separations are 2.829(1) and 3.158(1) Å, respectively. The intramolecular hydrogen bonds [O(1)−H(1D)···O(5) 2.689(2) Å] between an OH group of H_2tea and the tma oxygen atom O5[20] provide further reinforcement of the ∼Cu_2/Na−tma−Cu_2/Na∼ motifs. Additionally, both O6 oxygen atoms[20] of the uncoordinated COO group in tma act as hydrogen bond acceptors bridging between OH groups (O3) of H_2tea from neighboring units [O(3)−H(3D)···$O(6)^{vi}$ 2.743(2) Å], thus multiply linking the neighboring ∼Cu_2/Na−tma−Cu_2/Na∼ motifs with formation of the double hydrogen-bonded chains (Figure S1 in the Supporting Information).

(20) And their symmetry equivalents.

Table 2. Selected Bond Lengths (Angstroms) and Angles (Degrees) for **1**−**4**[a]

		1	
Cu(1)−O(1)	1.930(5)	O(1)−Cu(1)−O(22)	91.38(19)
Cu(1)−O(10)	2.566(7)	O(12)−Cu(1)−O(12)^{i}	80.30(15)
Cu(1)−O(12)	1.948(4)	O(10)−Cu(1)−O(12)	80.50(15)
Cu(1)−O(22)	2.510(6)	Cu(1)−O(10)−Cu(1)^{i}	66.0(2)
Cu(1)−N(1)	2.021(5)	Cu(1)−O(12)−Cu(1)^{i}	91.27(15)
Cu(1)−O(12)^{i}	1.959(4)		
		2[b]	
Cu(1)−O(3)	1.936(4)	Cu(1)−O(5)	2.577(4)
Cu(1)−O(1)	1.966(3)	O(1)−Cu(1)−O(6)	89.89(13)
Cu(1)−O(4)	1.953(3)	O(3)−Cu(1)−O(4)	81.48(14)
Cu(1)−N(1)	2.039(4)	Cu(1)−O(3)−Cu(2)	96.16(15)
Cu(1)−O(6)	2.459(4)	Cu(2)−O(4)−Cu(1)	95.70(15)
		3	
Cu(1)−O(2)	1.9521(15)	O(1)−Cu(1)−O(4)	92.21(6)
Cu(1)−O(3)	2.4024(16)	O(1)−Na(1)−O(1)^{ii}	154.68(10)
Cu(1)−O(4)	1.9609(15)	O(1)−Na(1)−O(7)	116.99(6)
Cu(1)−N(1)	2.0415(18)	O(7)−Na(1)−O(7)^{ii}	84.50(10)
Na(1)−O(1)	2.3528(16)	O(1)−Na(1)−O(2)	78.05(6)
Na(1)−O(7)	2.387(2)	O(2)−Na(1)−O(2)^{ii}	56.53(7)
Na(1)−O(2)	2.6196(19)	Cu(1)^{ii}−O(2)−Cu(1)	92.93(6)
O(2)^{ii}−Cu(1)−O(2)	78.97(7)	Cu(1)−O(2)−Na(1)	86.07(5)
		4a	
Cu(1)−O(8B)	1.9530(19)	Cu(2)−O(14)^{iii}	1.9607(16)
Cu(1)−O(14)	1.9595(17)	Cu(2)−O(16)^{iii}	2.5549(19)
Cu(1)−O(22)	1.9248(16)	Cu(2)−O(22)^{iii}	1.9449(17)
Cu(1)−O(24)	2.488(2)	Cu(2)−N(1)^{iii}	2.079(2)
Cu(1)−O(26)	2.613(2)	O(14)−Cu(1)−O(22)	80.62(7)
Cu(1)−N(2)	2.056(2)	O(14)^{iii}−Cu(2)−O(22)^{iii}	80.10(7)
Cu(2)−O(1A)	1.9520(18)	Cu(1)−O(14)−Cu(2)^{iv}	95.84(7)
Cu(2)−O(12)^{iii}	2.328(2)	Cu(1)−O(22)−Cu(2)^{iv}	97.50(7)
		4b	
Cu(1)−O(4)	1.943(4)	Na(1)−O(5)	2.359(5)
Cu(1)−O(2)	1.945(3)	O(2)−Cu(1)−O(7)	80.07(15)
Cu(1)−O(7)	1.956(4)	O(4)−Cu(1)−O(1)	91.19(15)
Cu(1)−N(1)	2.031(5)	O(2)−Cu(2)−O(7)	80.57(15)
Cu(1)−O(1)	2.404(4)	Cu(2)−O(2)−Cu(1)	94.50(15)
Cu(1)−O(3)	2.589(8)	Cu(2)−O(7)−Cu(1)	94.06(15)
Cu(2)−O(2)	1.939(4)	O(5)−Na(1)−O(12)	112.6(2)
Cu(2)−O(7)	1.942(3)	O(5)−Na(1)−O(11)	87.05(19)
Cu(2)−O(9)	1.950(4)	O(5)−Na(1)−O(1)^{v}	160.66(17)
Cu(2)−N(2)	2.035(6)	O(11)−Na(1)−O(1)^{v}	79.87(17)
Cu(2)−O(8)	2.416(6)	O(5)−Na(1)−O(11)^{v}	87.58(17)
Cu(2)−O(6)	2.647(8)	O(11)−Na(1)−O(11)^{v}	88.36(18)
Na(1)−O(13)	2.342(7)	O(1)^{v}−Na(1)−O(11)^{v}	77.94(17)
Na(1)−O(12)	2.384(6)	Na(1)−O(11)−Na(1)^{v}	91.64(18)
Na(1)−O(11)	2.408(5)	Cu(1)−O(1)−Na(1)^{v}	123.73(19)
Na(1)−O(1)^{v}	2.421(5)		

[a] Symmetry transformations used to generate equivalent atoms: (i) $1-x, y, {}^1/_2-z$; (ii) $-x, y, -z+{}^1/_2$; (iii) $x, {}^1/_2-y, {}^1/_2+z$; (iv) $x, {}^1/_2-y, -{}^1/_2+z$; (v) $-x+1, -y+1, -z+2$. [b] Bond distances and angles around Cu2 are almost equal, within 3σ, to those around Cu1 and thus are not given.

$[Cu_2(H_2tea)_2(\mu_2\text{-ipa})]_n\cdot n H_2O$ (4a). The crystal structure of **4a** (part d of Figure 1) is composed of typical dimeric $[Cu_2(H_2tea)_2]^{2+}$ units linked by bridging μ_2-ipa moieties forming linear metal−organic chains (part d of Figure 2). In general, **4a** shows some common features with those of **2** and **4b** (below) and thus is not discussed further.

$[Cu_2(H_2tea)_2\{\mu\text{-}Na(H_2O)_3\}(\mu_3\text{-ipa})]_n(NO_3)_n\cdot 0.5nH_2O$ (4b). Although the crystal structure of **4b** (part e of Figure 1) also reveals the linkage of an aqua sodium moiety to the dimeric copper triethanolaminate $[Cu_2(H_2tea)_2]^{2+}$ unit, the binding mode and type are different from those in **3**. Hence, in **4b** the $[Cu_2(H_2tea)_2]^{2+}$ units are interconnected by isophthalate bridges, forming two parallel $\sim Cu_2-ipa-Cu_2\sim$ chains, which are further interlinked by dimeric aqua sodium $[Na_2(\mu\text{-}H_2O)_2(H_2O)_4]^{2+}$ moieties, leading to the formation of double metal−organic chains (part e of Figure 2). The $[Cu_2(H_2tea)_2]^{2+}$ unit is asymmetric, and the bonding parameters around the Cu1 and Cu2 atoms are slightly different (Table 2) but comparable to those of **3** and **4a**. Only one OH group (O1) from two H_2tea moieties of the $[Cu_2(H_2tea)_2]^{2+}$ unit acts in a bridging mode and is additionally bound to the sodium ion [Na1−O1^{v} 2.421(5) Å]. The latter is also connected to the carboxylate oxygen (O5) of one COO group of isophthalate [Na1−O5 2.359(5) Å], thus providing the dual lacing of the $\sim Cu_2-ipa-Cu_2\sim$ chains with the corresponding O5−Na1−O1^{v} angle of 160.66(17)°. The distorted octahedral geometry of the sodium ion is completed by two terminal (O12, O13) and two bridging (O11) water molecules with the corresponding Na1−O12, Na1−O13, and Na1−O11 bond lengths of 2.384(6), 2.342(7), and 2.408(5) Å, respectively. The symmetry-equivalent Na1 atoms generate the centrosymmetric $[Na_2(\mu\text{-}H_2O)_2(H_2O)_4]^{2+}$ moiety, in which the square-type $[Na_2(\mu\text{-}H_2O)_2]$ unit is planar. The latter constitutes the central part of an unusual heterometallic copper/sodium core $[\{Cu_2(\mu\text{-}O)_2\}_2(\mu\text{-}O)_2Na_2(\mu\text{-}H_2O)_2]^{6+}$, which possesses a sea-horse-shaped geometry (part d of Figure 3), with the shortest Cu···Cu, Na···Na, and Cu···Na separations of 2.8524(9), 3.495(5), and 4.254(7) Å, respectively. The overall positive charge (+6) of that core is balanced by two isophthalate(2-) ligands acting in a μ_3-bridging mode and two nitrate ions. Several intramolecular hydrogen bonds (part e of Figure 1) provide an additional stabilization within the $[Cu_2(H_2tea)_2]^{2+}$ unit [O(6)−H(6O)···O(3) 2.771(6) Å] and $\sim Cu_2-ipa-Cu_2\sim$ chains [O(1)−H(1O)···O(5) 2.691(5), O(8)−H(8O)···O(10) 2.658(7) Å], as well as their further tying with the $[Na_2(\mu\text{-}H_2O)_2(H_2O)_4]^{2+}$ blocks [O(11)−H(11E)···O(7)^{ii} 2.771(6), O(12)−H(12F)···O(2)^{ii} 2.856(8) Å] (Table 3).

Comparison of Polymeric Architectures in 1−4 and Related Compounds. The schematic representation of polymeric architectures in the new **1**−**4** and the related coordination polymers $[Cu_2(H_2tea)_2(\mu_2\text{-tpa})]_n\cdot 2nH_2O$ (**A**)[7a] and $[Cu_2(H_2tea)_2\{\mu_3\text{-}Na_2(H_2O)_4\}(\mu_6\text{-pma})]_n\cdot 10nH_2O$ (**B**)[7b] (which we have previously synthesized and are now indicated for comparative purposes) is shown in Scheme 3, whereas the selected corresponding metal−metal separations are given in Table 4. The drawings of Scheme 3 correspond to the metal−organic chains of Figure 2. Additional crystal packing diagrams depicting the relative arrangement and architecture of four metal−organic chains in the crystal cells of **1**−**4** are shown in Figures S2−S6 of the Supporting Information.

In spite of the fact that the solid-state structures of all of the above-mentioned compounds reveal 1D metal−organic chains built from the $\{Cu_2(\text{aminopolyalcohol})_2\}^{2+}$ or $\{Cu_2Na(\text{aminopolyalcohol})_2\}^{3+}$ units and various benzenepolycarboxylate spacers, the relative arrangements and architectures of those chains are distinct in each compound (Scheme 3). Hence, in **A** the metal−organic chains derived from the $[Cu_2(H_2tea)_2]^{2+}$ units and terephthalate spacers adopt a linear-type geometry, possessing neighboring chains shifted aflat relatively to each other as depicted in Scheme 3. In

Table 3. Hydrogen Bonding Distances [d(D···A), Å] in **1**−**4**[a]

com-pound	within H_2O cluster		between H_2O clusters (or crystallization water) and metal−organic chains		within metal−organic chains		symmetry codes
	D−H···A	d(D···A)	D−H···A	d(D···A)	D−H···A	d(D···A)	
1	O(10)−H(10)···O(20)^{i}	2.758(7)	O(20)−H(20A)···O(12)^{ii}	2.756(7)	O(22)−H(22)···O(2)	2.677(7)	(i) $1-x, y, 1/2-z$; (ii) $1-x, -1+y, 1/2-z$
2	O(11)−H(11O)···O(14B)	2.568(15)	O(14B)−H(15O)···O(6)^{i}	2.765(10)	O(6)−H(6O)···O(2)	2.677(5)	(i) $-x+1, -y, -z+1$; (ii) $x+1/2, -y+1/2, z-1/2$
	O(11)−H(11O)···O(14A)	3.129(16)	O(14A)−H(14O)···O(4)^{i}	2.808(10)	O(7A)−H(7O)···O(10)	2.518(16)	
	O(14B)−H(15P)···O(11)^{ii}	2.685(14)	O(12)−H(12P)···O(2)	2.877(6)	O(7B)−H(7P)···O(10)	2.750(12)	
	O(14A)−H(14P)···O(11)	3.129(16)	O(13)−H(13P)···O(10)^{i}	2.816(6)	O(8)−H(8O)···O(5)	2.716(5)	
	O(12)−H(12O)···O(11)	2.728(10)	O(5)−H(5O)···O(13)^{ii}	2.678(5)			
	O(13)−H(13O)···O(12)	2.708(6)					
3	O(7)−H(7E)···O(8)^{i}	2.722(3)	O(7)−H(7D)···O(5)^{iv}	2.844(2)	O(1)−H(1D)···O(5)	2.689(2)	(i) $-x, y, -z+1/2$; (ii) $-x+1/2, y-1/2, z-1$; (iii) $x, -y, z+1/2$; (iv) $-x, -y, -z+1$; (v) $-x, -y+1, -z+2$; (vi) $x, -y+1, z-1/2$
	O(8)−H(8D)···O(9)^{i}	2.750(3)	O(9)−H(9D)···O(5)	2.890(2)	O(3)−H(3D)···O(6)^{vi}	2.743(2)	
	O(8)−H(8E)···O(10)^{ii}	2.790(3)	O(10)−H(10D)···O(6)^{v}	2.851(2)			
	O(9)−H(9E)···O(7)^{iii}	2.907(3)	O(10)−H(10E)···O(6)	2.812(2)			
4a			O(10)−H(10B)···O(14)	2.783(3)	O(16)−H(16)···O(1B)^{ii}	2.596(3)	(i) $1/2-x, -1/2+y, z$; (ii) $x, 1/2-y, -1/2+z$; (iii) $1/2-x, 1/2+y, z$
			O(10)−H(10A)···O(26)	2.840(3)	O(26)−H(26)···O(8A)	2.612(3)	
			O(24) −H(24)···O(10)^{i}	2.698(3)	O(12)−H(12)···O(16)^{iii}	2.702(3)	
4b	O(13)−H(13E)···O(14)	2.753(11)	O(3)−H(3O)···O(18)^{i}	3.02(2)	O(1)−H(1O)···O(5)	2.691(5)	(i) $x, -y+1/2, z-1/2$; (ii) $-x+1, -y+1, -z+2$; (iii) $x+1, y, z$
	O(13)−H(13F)···O(17)	2.760(15)	O(3)−H(3O)···O(19)^{i}	3.186(19)	O(6)−H(6O)···O(3)	2.562(13)	
	O(11)−H(11F)···O(19)^{ii}	3.233(17)	O(20)−H(20E)···O(10)	2.830(12)	O(8)−H(8O)···O(10)	2.658(7)	
	O(12)−H(12E)···O(20)^{iii}[b]	2.756(13)			O(11)−H(11E)···O(7)^{ii}	2.771(6)	
					O(12)−H(12F)···O(2)^{ii}	2.856(8)	

[a] Full hydrogen bond geometry parameters are given in the Supporting Information (Tables S1−S5). [b] An additional short contact [O(15)···O(20)^{ii} 2.83(2) Å] is also found between nitrate oxygen (O15) and crystallization water molecule (O20).

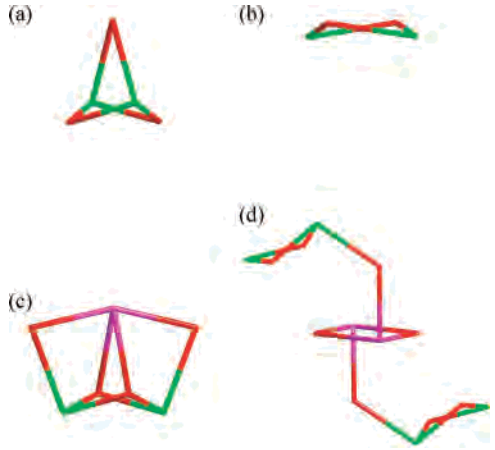

Figure 3. Capped sticks structural representations showing (a) cocked-hat-like [$Cu_2(\mu$-O)$_2(\mu$-$H_2O)$] core in **1**, (b) twisted-square [$Cu_2(\mu$-O)$_2$] core in **2** and **4a**, (c) crown-like [$Cu_2(\mu_2$-O)$_2(\mu$-O)$_2$Na] core in **3**, and (d) sea-horse-shaped [{$Cu_2(\mu$-O)$_2$}$_2(\mu$-O)$_2$Na$_2(\mu$-$H_2O)_2$] core in **4b**. Hydrogen atoms are omitted for clarity. Copper, green; oxygen, red; sodium, purple.

contrast, the metal−organic chains of **1** built from the $[Cu_2(Hmdea)_2]^{2+}$ units and the same tpa spacers are symmetrical and show a wavelike geometry with up−down alternate dimeric copper units. The different zigzag-type motifs with vertically flipping ipa spacers are found in the crystal structure of **2** that comprises the $[Cu_2(H_2tipa)_2]^{2+}$ fragments. The same vertically flipping ipa spacers can be seen in **4a**, which however does not possess an aflat shift of metal−organic chains, thus defining their slightly wavy (nearly linear) shape. Within the ∼Cu_2/Na−tma−Cu_2/Na∼ motifs of **3**, the trimesate spacers are oriented in a similar manner, leading to the linear chains, which are flipped vertically and shifted aflat relatively to each other. Although a similar arrangement of two neighboring ∼Cu_2−ipa−Cu_2∼ chains is also detected in **4b**, its overall architecture is different due to the additional inclusion of the bridging $[Na_2(\mu$-$H_2O)_2$-$(H_2O)_4]^{2+}$ moieties, leading to the linear double copper/sodium chains. **B** with the pma spacer instead of ipa possesses related but more-intricate 2D architecture, owing to the infinite character of the ∼Na_2−pma−Na_2∼ motifs. In all of the compounds, the shortest Cu−spacer−Cu separation within one metal−organic chain differs from 9.590 to 11.240 Å, whereas the shortest Cu···Cu distance between two neighboring chains depicted in Scheme 3 varies from 6.784 to 10.184 Å (Table 4). In general, both types of main chelating ligands and spacers significantly affect the resulting polymeric patterns of all of the compounds synthesized by the current self-assembly approach (Scheme 1).

Hydrogen-Bonded Frameworks and Water Clusters. Additional features of solid-state structures of all of the 1D frameworks **1**−**4** consist in the presence of crystallization water molecules, which extensively interact via plenty of intermolecular hydrogen bonds with the host metal−organic matrix, thus contributing to a structure-stabilizing effect and leading to the formation of extended 2D or 3D hydrogen-bonded supramolecular assemblies (Figure S7 in the Supporting Information). In **1**−**3**, the intercalated crystallization and coordinated water molecules are further associated by hydrogen bonding contacts, resulting in the formation of various types of water clusters (Figure 4), whereas in **4b** the crystallization water interacts with nitrate ions. Additional crystal packing diagrams of **1**−**3** including the space filling representation of intercalated water clusters are given in the Supporting Information as Figures S8−S12.

Water Trimers in 1. Two symmetry-generated crystallization water molecules (O20) in the unit cell of **1** are hydrogen bonded [O10−H10···O20^{i} 2.719(8) Å] to coordinated water (O10), thus forming the discrete acyclic water trimers (part a of Figure 4), which can be classified within the D3-type according to the systematization introduced by Infantes et al.[9b,c] These trimers occupy a free space in the

Scheme 3. Schematic Representation of Polymeric Architectures in **1**−**4**,[a] **A**,[7a] and **B**[7b]

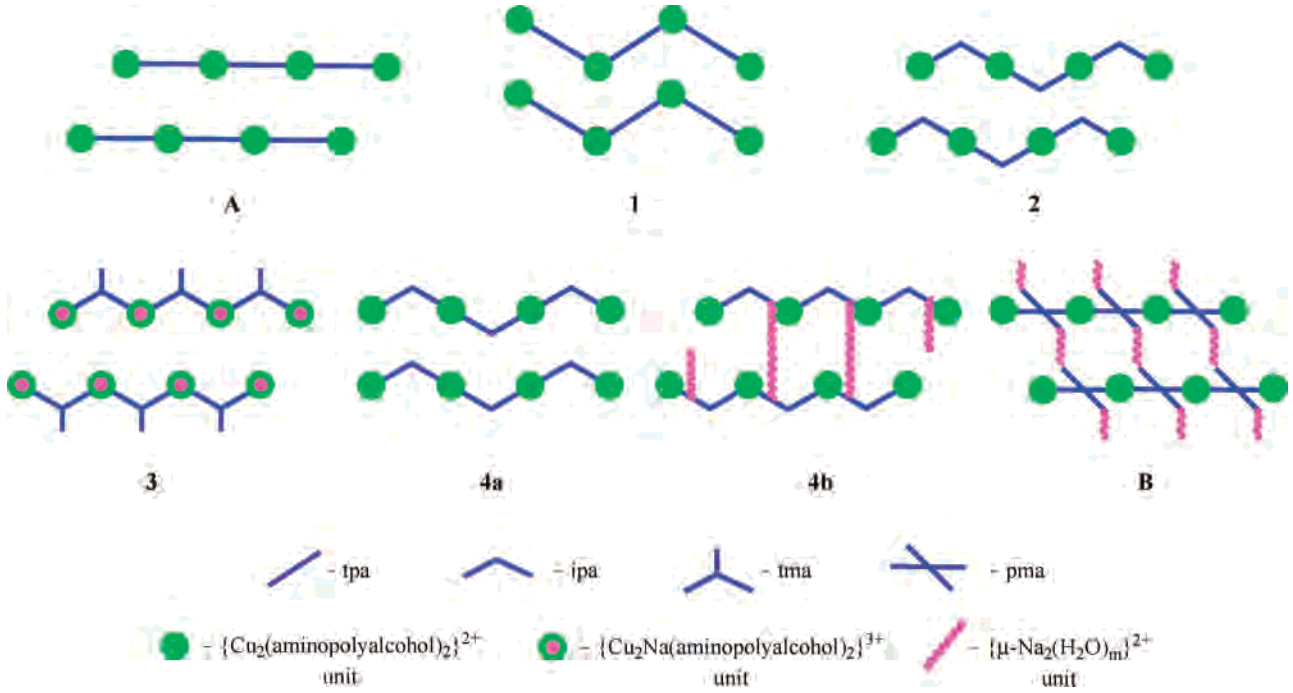

[a] Those for **1**−**4** correspond to the metal−organic chains depicted in Figure 2.

Table 4. Selected Metal−Metal Separations (Angstroms) in **1**−**4**[a]

compound	Cu···Cu (dimeric unit)	Cu-spacer-Cu (within one chain)[b]	Cu···Cu (neighboring chains)	Cu···Na	Na···Na (dimeric unit)
1	2.793(6)	11.059	6.977		
2	2.886(1)	9.590	10.184		
3	2.829(1)	10.752	9.483	3.158(1)	
4a	2.909(1)	10.874	6.784		
4b	2.852(1)	10.694	8.319[c]	4.254(7)	3.495(5)
A[d]	2.905(1)	11.168	7.498		
B[d]	2.964(3)	11.240	8.722	3.679	3.398(4)

[a] The values correspond to shortest separations within those metal−organic chains represented in Scheme 3 and Figure 2. [b] Spacer corresponds to benzenepolycarboxylate. [c] Value within one double metal−organic chain. [d] Given for comparative purposes.

crystal cell and are doubly connected [O20−H20A···O12^{ii} 2.759(7) Å] to neighboring wavelike 1D metal−organic chains, sewing them together and forming the 2D sheets if seen along the *a* axis (part a of Figure S7). The O···O distances of 2.719(8) Å within the water trimers are comparable to those found in the regular ice (ca. 2.74 Å)[21a] and others described acyclic $(H_2O)_3$ clusters trapped by various metal−organic matrixes.[21]

Water Octamers in 2. The unit cell of **2** reveals the presence of four (one of them is partially lost) crystallization water molecules (O11−O14), which are associated to form symmetry-generated finite $(H_2O)_8$ clusters composed of a cyclic tetrameric core (O11···O14···O11···O14) and two pendent water dimers (O12···O13) (part b of Figure 4). They can be ascribed to the R4-type according to the above-mentioned classification.[9b,c] Within the $(H_2O)_8$ cluster, the

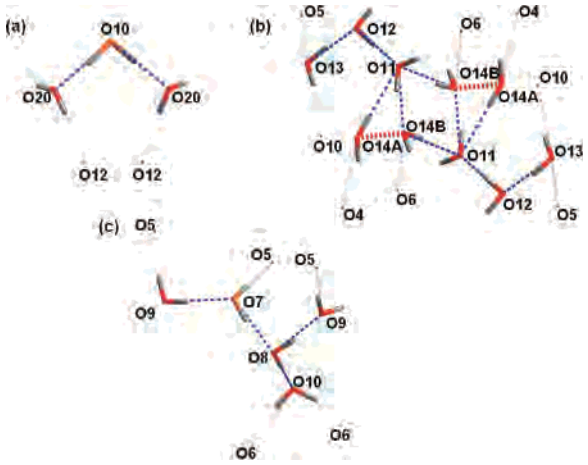

Figure 4. Perspective representations of water clusters found in the crystal cells of **1** (a), **2** (b), and **3** (c), with hydrogen bonding network (blue dashed lines) and atom labeling scheme. Crystallization water oxygen atoms, red; coordinated water oxygen atoms, orange. Hydrogen bonds within water clusters, blue clear-cut dashed lines; hydrogen bonds between water clusters and metal−organic chains, blue dingy dashed lines. Short contacts between disordered over two sites water molecules are shown as red dotted lines.

average O···O contact of ca. 2.82 Å (Table 3) is comparable to one found in liquid water (i.e., 2.85 Å).[9d] The geometry of the thus identified $(H_2O)_8$ cluster appears to be rather unusual but should be considered rather cautiously in view of the disordered character of the O14 water molecules. Other types of related (i) cyclic $(H_2O)_4$ clusters,[22] (ii) cyclic tetramers with two dangling $(H_2O)_n$ ($n = 1$ or 3) groups,[5a] or (iii) octamers with, for example, cyclic $(H_2O)_6$ cores and

(21) (a) Ghosh, S. K.; Ribas, J.; Bharadwaj, P. K. *Cryst. Growth Des.* **2005**, *5*, 623. (b) Shivaiah, V.; Das, S. K. *Inorg. Chem.* **2005**, *44*, 8846. (c) Ghosh, S. K.; Bharadwaj, P. K. *Inorg. Chem.* **2005**, *44*, 5553. (d) Zhu, L. N.; Ou-Yang, Y.; Liu, Z. Q.; Liao, D. Z.; Jiang, Z. H.; Yan, S. P.; Cheng, P. *Z. Anorg. Allg. Chem.* **2005**, *631*, 1693.

(22) (a) Xing, Y. H.; Yuan, H. Q.; Zhang, Y. H.; Zhang, B. L.; Bai, F. Y.; Niu, S. Y. *Synth. React. Inorg. Met.* **2006**, *36*, 641. (b) Sun, Y. Q.; Zhang, J.; Ju, Z. F.; Yang, G. Y. *Aust. J. Chem.* **2005**, *58*, 572. (c) Long, L. S.; Wu, Y. R.; Huang, R. B.; Zheng, L. S. *Inorg. Chem.* **2004**, *43*, 3798.

two dangling H_2O molecules,[5a,23] have been experimentally detected in metal−organic frameworks. In **2**, water octamers occupy holes between the $[Cu_2(H_2tipa)_2]^{2+}$ units of the neighboring ∼Cu_2−ipa−Cu_2∼ chains and additionally interact via multiple hydrogen bonds with these metal−organic chains, extending them to a second dimension and resulting in the 2D framework if seen, for example, along the *c* axis (part b of Figure S7).

Infinite 1D Water Chains in 3. In the crystal cell of **3**, three symmetry nonequivalent crystallization H_2O molecules (O8, O9, and O10) as well as a water ligand (O7) from the $[Na(H_2O)_2]^+$ moiety are clustered, forming the acyclic O9···O7···O8···O10 water tetramers (part c of Figure 4), which are additionally interconnected via the O(8)−H(8D)···O(9)^{i} hydrogen bond, thus generating the infinite-branched 1D water chains (Figure S8 in the Supporting Information). They can be classified within the C4 type according to the above-mentioned systematization.[9b,c] The repeating period of these chains is ca. 6.75 Å, whereas the O···O contacts differ from 2.722(3) to 2.907(3) Å [av 2.792(3) Å] (Table 3), the values being within the range found in other 1D polymeric water chains trapped within copper-containing supramolecular assemblies.[24] The crystal packing diagram of **3** (90° rotated view along the *a* axis) shows two metal−organic chains with interchain cavities filled by two layers of water chains (part c of Figure S7). They act as multiple hydrogen bond donors to trimesate oxygen atoms [i.e., O(7)···O(5)^{iv}, O(9)···O(5), O(10)···O(6), and O(10)···O(6)^{v} interactions] (Table 3), leading to the 3D hydrogen-bonded supramolecular pattern.

Water-Nitrate Interactions in 4b. The crystal structure of **4b** reveals the presence of two crystallization water molecules (O20) and four nitrate ions (N3, N4) per unit cell. Although they possess a substantial degree of disorder and thus should be considered cautiously, one should mention their interactions (Table 3) with all water ligands from the $[Na_2(\mu\text{-}H_2O)_2(H_2O)_4]^{2+}$ moiety generating the $\{[(H_2O)_4(NO)_3]^-\}_n$ aggregates. The latter are disposed between ∼Cu_2-ipa-Cu_2∼ motifs if seen, e.g., along the *b* axis and hydrogen bonded to H_2tea and isophthalate oxygen atoms (i.e., O3 and O10, respectively) providing an additional reinforcement of the metal−organic matrix with formation of the 3D H-bonded framework (Figure S7e). Examples of identified water−nitrate clusters within the crystal hosts of Co and Ag compounds have been recently reported.[25]

Magnetic properties. The magnetic properties of compounds **1**, **2**, **3** and **4a**, under the form of $\chi_M T$ vs T plot (χ_M being the molar susceptibility per two copper(II) ions), are shown in Figure 5. For all of the compounds, $\chi_M T$ at room temperature is above that expected for two magnetically isolated spin doublets and, upon cooling, $\chi_M T$ continuously increases to reach a plateau (or a maximum) before decreasing at lower temperatures. The values of $\chi_M T$ in the maximum and in the plateau correspond to a $S = 1$ spin state. These features are indicative of the occurrence of a moderately strong ferromagnetic intramolecular coupling between the copper(II) ions together with weak antiferromagnetic intermolecular interactions and/or zero-field splitting effects that account for the decrease of $\chi_M T$ at low temperatures. Having in mind the dinuclear structure of the compounds, the magnetic data were analyzed by means of the isotropic spin Hamiltonian $\boldsymbol{H} = -J(S_1S_2)$ that leads to the Bleaney−Bowers expression for two interacting spin doublets, eq (1),[10] where J is the intramolecular exchange coupling constant, g is the Landé factor, β is the Bohr magneton, and k is the Boltzman's constant. A zero-field splitting term (D) and a Curie−Weiss parameter (θ) was also considered.[10]

$$\chi_M = \frac{N\beta^2 g^2}{3kT}\left[\frac{6}{3 + \exp(-J/kT)}\right] \qquad (1)$$

Best-fit parameters are shown in Table 5. The values obtained for θ confirm the occurrence of weak intermolecular antiferromagnetic coupling (due to the large size of the benzenepolycarboxylate spacers), and the values obtained for D are within the range of similar copper(II) dinuclear complexes.[11] However, the decrease of $\chi_M T$ at low temperatures is more likely due to interdimer antiferromagnetic interactions, and these results can be improved. The shape of the $\chi_M T$ versus T plot and the high values found for the exchange coupling constants with the Bleaney−Bowers model allows a different approach to describe the magnetic behavior of **1**−**4a**. The intramolecular magnetic coupling of the dinuclear units is very strong (as can be seen in Table 5) and at low temperatures, when the intermolecular interactions show their influence, the copper(II) ions are completely coupled and the total spin of the dimer is 1. Under these conditions, the magnetic behavior of **1**−**4a** can be described with a model of 1D chains of dinuclear units (Scheme 3), denoted as P, which are antiferromagnetically coupled through the benzenepolycarboxylate ligands. The value of the spin of the P units, S_p, is a function of J and T, being given by eq 2.[26]

$$S_p(S_p + 1) = [6/3 + \exp(-J/kT)] \qquad (2)$$

At low temperatures, S_P is high enough to be considered as a classical spin, and the magnetic data of **1**−**4a** can be

(23) (a) Prasad, T. K.; Rajasekharan, M. V. *Cryst. Growth Des.* **2006**, *6*, 488. (b) Ghosh, S. K.; Bharadwaj, P. K. *Inorg. Chim. Acta* **2006**, *359*, 1685. (c) Ma, B. Q.; Sun, H. L.; Gao, S. *Chem. Commun.* **2005**, 2336.

(24) (a) Hu, N.-H.; Li, Z.-G.; Xu, J.-W.; Jia, H.-Q.; Niu, J.-J. *Cryst. Growth. Des.* **2007**, *7*, 15. (b) Du, M.; Jiang, X. J.; Zhao, X. J.; Cai, H.; Ribas, J. *Eur. J. Inorg. Chem.* **2006**, 1245. (c) Song, J. F.; Lu, J.; Chen, Y.; Liu, Y. B.; Zhou, R. S.; Xu, X. Y.; Xu, J. Q. *Inorg. Chem. Comm.* **2006**, *9*, 1079. (d) Wang, X.; Ranford, J. D.; Vittal, J. J. *J. Mol. Struct.* **2006**, *796*, 28. (e) Lou, B. Y.; Jiang, F. L.; Yuan, D. Q.; Wu, B. L.; Hong, M. C. *Eur. J. Inorg. Chem.* **2005**, 3214. (f) Liu, P.; Wang, Y. Y.; Li, D. S.; Ma, H. R.; Shi, Q. Z.; Lee, G. H.; Peng, S. M. *Inorg. Chim. Acta* **2005**, *358*, 3807.

(25) (a) Li, Z. G.; Xu, J. W.; Via, H. Q.; Hu, N. H. *Inorg. Chem. Comm.* **2006**, *9*, 969. (b) Robin, A. Y.; Doimeadios, J. L. S.; Neels, A.; Slenters, T. V.; Fromm, K. M. *Inorg. Chim. Acta* **2007**, *360*, 212.

(26) (a) Lloret, F.; Julve, M.; Ruiz, R.; Journaux, Y.; Nakatani, K.; Kahn, O.; Sletten, J. *Inorg. Chem.* **1993**, *32*, 27. (b) Lloret, F.; Ruiz, R.; Julve, M.; Faus, J.; Journaux, Y.; Castro, I.; Verdaguer, M. *Chem. Mater.* **1992**, *4*, 1150. (c) Lloret, F.; Ruiz, R.; Cervera, B.; Castro, I.; Julve, M.; Faus, J.; Real, J. A.; Sapiña, F.; Journaux, Y.; Colin, J. C.; Verdaguer, M. *Chem. Commun.* **1994**, 2615. (d) Thomson, L. K.; Tandon, S. S.; Lloret, F.; Julve, M.; Cano, J. *Inorg. Chem.* **1997**, *36*, 3301.

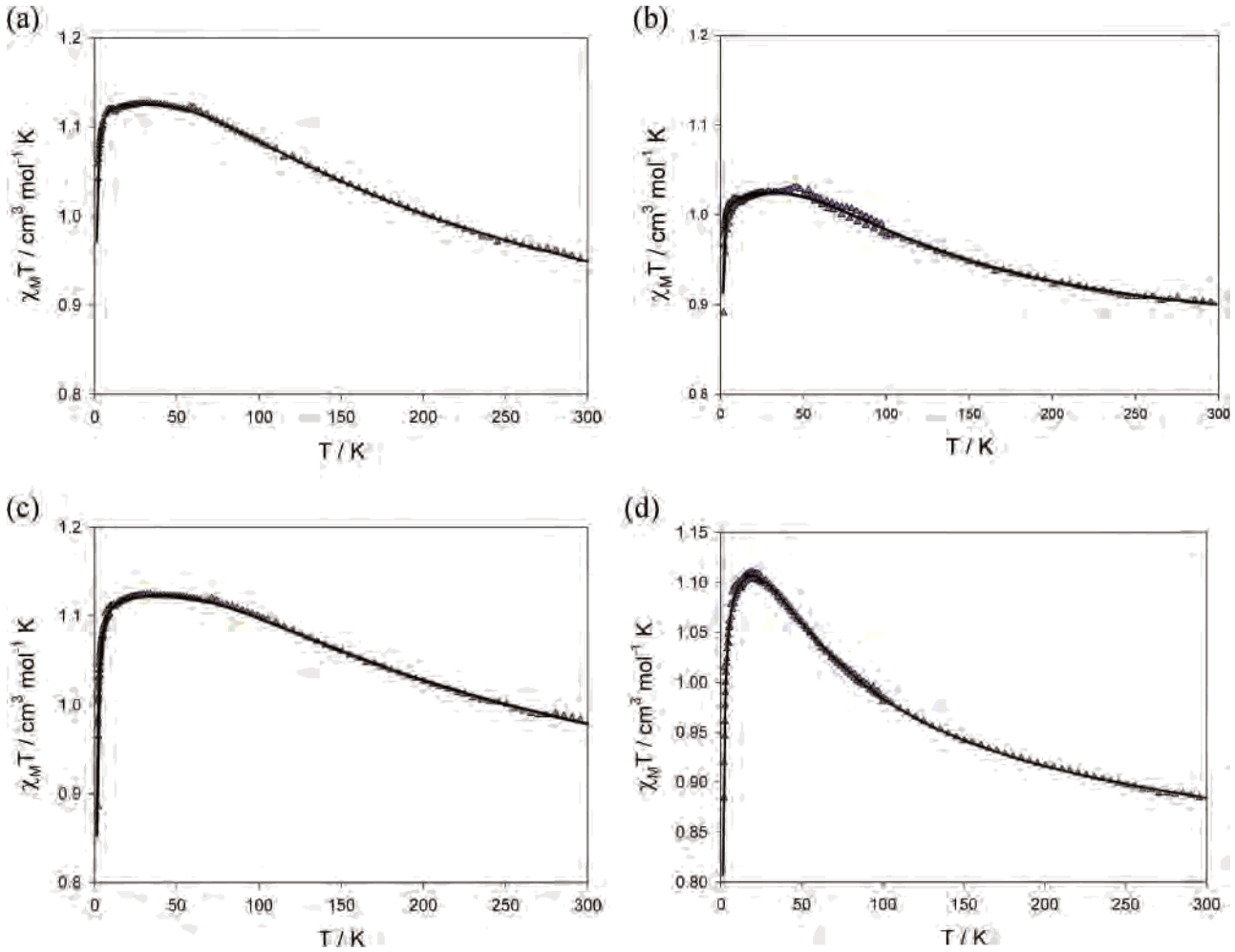

Figure 5. $\chi_M T$ versus T plot for **1** (a), **2** (b) **3** (c) and **4a** (d): Δ experimental data, (—) best-fit curve (text).

Table 5. Selected Magnetostructural Data for **1**−**4a**[a]

	Bleaney−Bowers model				Fisher model			Selected structural parameters			
compound	g	Θ	D	J	g_P	j_{eff}	J	Cu−O−Cu (deg)	τ (deg)	γ (deg)	pK_b
1	2.13(1)	−0.33(1)	1.21(3)	155(1)	2.13(1)	−0.08(1)	153(2)	91.31(15)	26.4(4)	24.4(1)	5.44
2	2.02(1)	−0.18(1)	1.3(1)	128(4)	2.02(1)	−0.10(1)	118(3)	95.92[b]	32.3(4)	13.5(1)	5.85
3	2.12(1)	−0.57(10)	1.78(8)	192(5)	2.13(1)	−0.14(1)	173(4)	92.93(6)	27.1(1)	18.5(1)	6.20
4a	2.12(1)	−1.15(14)	1.95(6)	60(2)	2.13(1)	−0.19(1)	60(1)	96.67[b]	31.9(1)	12.4(1)	6.20
A	2.16(1)	−0.15(2)	0.96(4)	97(1)	2.16(1)	−0.05(1)	94.9(6)	96.26(5)	45.12(1)	0.00(6)	6.20
B	2.13(1)	−0.22(6)	0.1(2)	22(1)	2.13(1)	−0.02(1)	22.3(3)	98.68(9)	44.7(7)	0.00(9)	6.20

[a] Weiss constant (θ/K), Landé factor (g), zero-field splitting (D/cm^{-1}), magnetic exchange coupling constant (J/cm^{-1}), effective coupling constant (j_{eff}/cm^{-1}), out-of-plane shift of the carbon atom of the alkoxo bridge (τ/deg), hinge distortion at the Cu_2O_2 core (γ/deg). Standard deviations are given in parentheses. [b] Averaged Values.

analyzed by means of the Fisher equation for a chain of classical spins S_P, eq 3,[10b] where u is given by eq 4, g_P stands for the Landé factor of the P dinuclear unit, and j_{eff} for the effective coupling constant among the P units.

$$\chi_M = \frac{N\beta^2 g_P{}^2}{3kT} S_P(S_P+1)\left[\frac{1+u}{1-u}\right] \quad (3)$$

$$u = \coth[j_{eff}S_P(S_P+1)/kT] - [kT/j_{eff}S_P(S_P+1)] \quad (4)$$

Least-square fitting of the data leads to the results shown in Table 5 together with those of the Bleaney−Bowers model. The calculated curves reproduce the experimental data for the whole temperature range explored. The values obtained for J are very similar for both models, but the low-temperature data are better described by the Fischer model, giving an accurate value for the interdimer interaction through the benzenepolycarboxylate ligand. The main difference is found in the coupling constant of **3** and may be due to overparametrization of the Bleaney−Bowers equation with the inclusion of D and θ. The values obtained for j_{eff} confirm that the interaction through the benzenepolycarboxylate ligands is very weak, in agreement with the large copper−copper separation. Additionally, the small value obtained validates the model, because this approach is only appropriate when the j_{eff}/J ratio is very small as it is for **1**−**4a**.

Scheme 4. Definition of the Out-of-Plane Shift of the Carbon Atom of the Alkoxo Bridge (τ) and the Hinge Distortion of the [$Cu_2(\mu_2\text{-}O)_2$] Core (γ)[a]

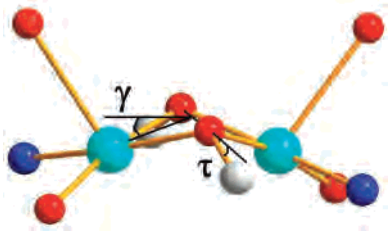

[a] Copper, light blue; oxygen, red; nitrogen, blue; carbon, light gray.

The magnetic properties of alkoxo-bridged copper(II) dinuclear complexes are usually explained on the basis of a correlation with the Cu−O−Cu angle; the smaller the angle the stronger the ferromagnetic coupling.[10,11] However, it should be noted that this is not an easy task for **1**−**4a** because their [$Cu_2(\mu_2\text{-}O)_2$] cores have very different structures (Figure 3), which makes it difficult to follow a simple correlation. **2** and **4a** have a very similar [$Cu_2(\mu_2\text{-}O)_2$] core, and their magnetic properties follow the general rule, the weaker ferromagnetic coupling corresponding to **4a** that shows the larger angle. This trend is also followed by **1** and **3** that have smaller angles than **2** and **4a** and thus exhibit stronger ferromagnetic couplings. On the other hand, there is an apparent abnormality for **1**, which having the smallest Cu−O−Cu bridging angle, does not display the strongest ferromagnetic coupling. To explain this behavior, we have analyzed other structural parameters, such as, the out-of-plane shift of the carbon atom of the alkoxo bridge (τ) or the hinge distortion of the [$Cu_2(\mu_2\text{-}O)_2$] core (γ) (Scheme 4).

These structural parameters are presented together with the results of the magnetic study in Table 5. τ is very similar for both compounds, and it does not allow us to perform any comparison and γ points toward **1** to have the strongest ferromagnetic character because a large distortion reduces the antiferromagnetic contribution.[11] (The magnetic coupling constant, J, can be expressed as the sum of two contributions, a ferromagnetic one and an antiferromagnetic one, with a competition between both, and what we observe is the sum of them: $J = J_F + J_{AF}$.)[10b] Nevertheless, the basicity of the terminal ligand also affects the exchange coupling constant (the antiferromagnetic contribution shows the same trend as that of the basicity of the terminal ligand), and the smaller ferromagnetic character of **1** can be explained by means of the more-basic character of the methyldiethanolamine with respect to the triethanolamine.[27] Another feature that may have an important effect is the additional bridging water molecule present in **1** that may mediate some antiferromagnetic coupling between the copper(II) ions, decreasing the overall ferromagnetic behavior. Most likely the combination of both effects makes the ferromagnetic character of **1** smaller than that of **3**. The magnetic properties of the compounds [$Cu_2(H_2tea)_2(\mu_2\text{-}tpa)]_n \cdot 2nH_2O$ (**A**)[7a] and [$Cu_2(H_2tea)_2\{\mu_3\text{-}Na_2(H_2O)_4\}(\mu_6\text{-}pma)]_n \cdot 10nH_2O$ (**B**)[7b] have also been studied and their magneto structural parameters are included in Table 5 for comparative purposes. We observe their magnetic coupling constant to be in agreement with those of **1**−**4a**. The smaller value of J corresponds to **B** that has the largest Cu−O−Cu angle, whereas the Cu−O−Cu angle of **A**, which is between those of **2** and **4a**, makes its magnetic coupling constant to be also between those of **2** and **4a**. **A** and **B** have an interesting structural restriction that makes γ to be zero that allows us to observe the important effect of the out-of-plane shift of the carbon atom of the alkoxo bridge (τ), which is the responsible for the ferromagnetic coupling in **B**.

Conclusions

This study shows the generality of the described self-assembly approach to the easy synthesis of 1D coordination polymers derived from various aminopolyalcoholate and benzenepolycarboxylate ligands. Their slight modification has a remarkable effect on the composition, structure, supramolecular features, and magnetic properties of the obtained copper or copper(II)/sodium(I) frameworks. The latter extend the still limited number of heteroligand copper-containing coordination polymers, bearing both aminopolyalcohol and benzenepolycarboxylate moieties.

The products exhibit unusual metal cores, which are interlinked by benzenepolycarboxyalate spacers, forming distinct wavelike (in **1**), zigzag (in **2**) or linear (in **3** and **4**) 1D polymeric metal−organic chains that are further extended via multiple hydrogen bonds to the 2D (in **1**, **2** and **4a**) or 3D (in **3** and **4b**) supramolecular frameworks. A main role in the formation and stabilization of the latter is played by intercalated water clusters such as water trimers, octamers, 1D chains, and disordered water−nitrate associates in **1**−**4b**, respectively. Hence, the work also extends the growing family of water clusters[9,21−25] hosted by metal−organic matrixes.

1 and **2** appear to constitute the first examples of transition-metal coordination polymers derived from the aminopolyalcohols triisopropanolamine and methyldiethanolamine,[2] thus opening their use in this field as cheap and commercially available chelating ligands. Moreover, the alkoxo-bridged dicopper(II) cores [$Cu_2(\mu\text{-}O)_2$] display a strong ferromagnetic coupling, which, in one of the compounds, appears to reach the highest value so far reported for copper(II) complexes with alkoxo bridges.

The strategy of self-assembly synthesis will be extended to build new multidimensional metal−organic frameworks, including highly correlated magnetic systems by joining the above ferromagnetically coupled dicopper(II) units with ligands that can transmit more efficiently the magnetic interaction.

Acknowledgment. This work has been partially supported by the Foundation for Science and Technology (FCT) and its POCI 2010 programme (FEDER funded) and by a HRTM Marie Curie Research Training Network (AQUACHEM

(27) (a) Hall, J. L.; Simmons, R. B.; Morita, E.; Joseph, E.; Gavlas, J. F. *Anal. Chem.* **1971**, *43*, 634. (b) Smith, R.; Martell, A. E. *Critical Stability Constants*; Plenum Press: New York, 1989; Vol. 6.

project, CMTN−CT-2003-503864). J.S. acknowledges the Servicio General de Medidas Magnéticas of the Universidad de La Laguna for the magnetic measurement facilities.

Supporting Information Available: X-ray crystallographic file in CIF format for the structure determinations of **1**−**4**, figures showing additional crystal packing diagrams and structural fragments of **1**−**4**, and tables with full hydrogen bond geometry parameters in **1**−**4**. This material is available free of charge via the Internet at http://pubs.acs.org.

IC701669X